Eur. Phys. J. E **30**, 371-377 (2009) DOI: 10.1140/epje/i2009-10535-2

Response of prestretched nematic elastomers to external fields

Andreas M. Menzel[1,a], Harald Pleiner[2,b], and Helmut R. Brand[1,2,c]

[1] Theoretische Physik III, Universität Bayreuth, 95440 Bayreuth, Germany
[2] Max Planck Institute for Polymer Research, P.O. Box 3148, 55021 Mainz, Germany

Received 21 July 2009 and Received in final form 20 October 2009
Published online: 5 December 2009 - ©EDP Sciences / Società Italiana di Fisica / Springer-Verlag 2009

Abstract. We investigate the response of prestretched nematic side-chain liquid single crystal elastomers to superimposed external shear, electric, and magnetic fields of small amplitude. The prestretching direction is oriented perpendicular to the initial nematic director orientation, which enforces director reorientation. Furthermore, the shear plane contains the direction of prestretch. In this case, we obtain a strongly decreased effective shear modulus in the vicinity of the onset and the completion of the enforced director rotation. For the same regions, we find that it becomes comparatively easy to reorient the director by external electric and magnetic fields. These results were derived using conventional elasticity theory and its coupling to relative director-network rotations.

PACS. 61.30.Vx Polymer liquid crystals – 61.30.Dk Continuum models and theories of liquid crystal structure – 61.30.Gd Orientational order of liquid crystals; electric and magnetic field effects on order

1 Introduction

Side-chain liquid single crystal elastomers (SCLSCEs) consist of crosslinked polymer backbones, to which mesogenic molecules are attached as side-groups via flexible spacer units [1]. Information about the state of liquid crystalline order at the time of crosslinking is imprinted into the materials [2,3]. In this way, through specific routes of synthesis, liquid crystalline order in a macroscopic monodomain is induced in SCLSCEs [4–6].

Since the first synthesis of nematic SCLSCEs was reported [4], many experiments have been performed to study their behavior in external fields. They revealed a unique material-specific property: a coupling of mechanical strain deformations to liquid crystalline order. For example, strain deformations of nematic SCLSCEs can induce reorientations of the director [4, 5, 7–9], and, vice versa, reorientations of the director can lead to elastic distortions [3,6,10,11]. Experiments performed include investigations on the stress-strain behavior [4,5,7–9], piezorheometric measurements of the linear shear response [12–14], as well as investigations of the electro-optical [6] and electro-mechanical [3, 10, 11] properties. In the latter case, the response to external electric fields has been studied mainly for nematic SCLSCEs swollen with low molecular weight liquid crystals.

As a recent development in this area, the materials are exposed to an external field of large amplitude to drive them into the nonlinear regime. Then, a second external field is superimposed. The small-amplitude response to this second external field is recorded under the influence of the first, large-amplitude external field. Current experimental work includes small-amplitude shear measurements [15] as well as dynamic light scattering measurements [16] on prestretched nematic SCLSCEs. In the latter case, essentially the response to externally imposed electromagnetic fields is recorded.

2 Geometries under investigation

Here, we investigate two geometries of this kind (fig. 1). In both cases, a nematic SCLSCE is considerably prestretched by an external strain field of amplitude A. The latter is applied in a direction $\hat{\mathbf{z}}$ perpendicular to the initial director orientation $\hat{\mathbf{n}}_\mathbf{0}$ ($\|\hat{\mathbf{x}}$). Simultaneously, the sample contracts laterally by amplitudes B ($\|\hat{\mathbf{x}}$) and C ($\|\hat{\mathbf{y}}$). To respect an approximately constant volume of the sample, C is expressed by A and B [17].

We noted above the material-specific coupling of mechanical deformations and director orientation. As a consequence, above a certain threshold strain A_c, the increasing stretching field A leads to a continuous reorientation of the director $\hat{\mathbf{n}}$ towards the stretching direction [4, 5, 7, 8]. We introduce the angle of director reorientation $\vartheta = \measuredangle(\hat{\mathbf{n}}_\mathbf{0}, \hat{\mathbf{n}})$. This process of director reorientation is connected to a decrease in the slope of the corresponding stress-strain curve [4, 5, 9]. In addition, the reorientation process induces shear deformations of amplitude S in the

[a] e-mail: andreas.menzel@uni-bayreuth.de
[b] e-mail: pleiner@mpip-mainz.mpg.de
[c] e-mail: brand@uni-bayreuth.de

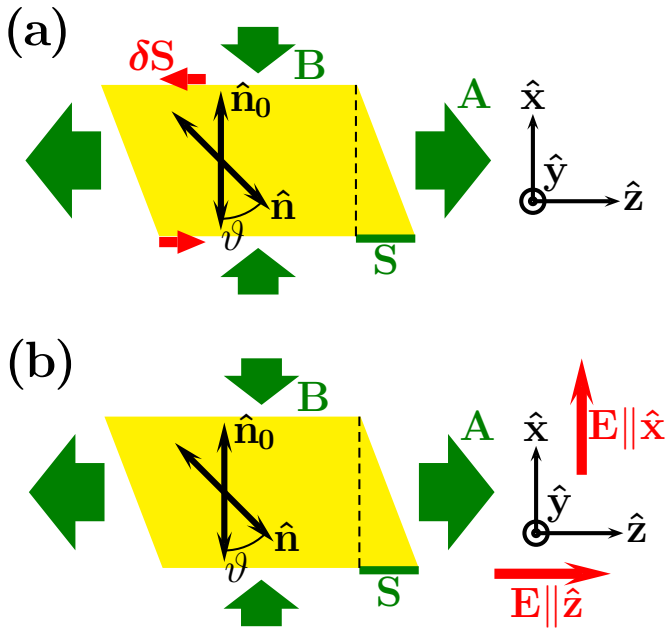

Fig. 1. Geometries of the set-ups under investigation. Here, A, B, and S denote the amplitudes of the corresponding elastic deformations. In the first case (a), an additional external shear deformation of small amplitude δS is imposed onto the prestretched material. In the second case (b), an additional external electric field $\mathbf{E}$ is applied either in $\hat{\mathbf{x}}$- or in $\hat{\mathbf{z}}$-direction.

plane of director rotation. We refer to our previous investigation on this kind of set-up [17] for a detailed discussion.

Here, we study the influence of an additional external field superimposed onto the external strain field A (fig. 1). First, we consider the effect of an additional shear deformation of small amplitude δS (fig. 1 (a)). The important point is that the corresponding shear plane coincides with the plane of director reorientation. In other words, δS acts to increase or decrease S. Secondly (fig. 1 (b)), an external electric field of magnitude E is applied either parallel to $\hat{\mathbf{n}}_\mathbf{0}$ ($\|\hat{\mathbf{x}}$), or along the stretching direction ($\|\hat{\mathbf{z}}$).

3 Macroscopic description

To investigate the respective set-up, we use the nonlinear continuum model introduced in ref. [17]. This model is based on the variables of relative rotations between the director $\hat{\mathbf{n}}$ and the network of crosslinked polymer chains [18,19]. In the nonlinear regime, two variables $\tilde{\mathbf{\Omega}}$ and $\tilde{\mathbf{\Omega}}^{\mathbf{nw}}$ are necessary to characterize these relative rotations [17]. (More precisely, we describe the relative rotations between $\hat{\mathbf{n}}$ and a second preferred direction $\hat{\mathbf{n}}^{\mathbf{nw}}$ imprinted into the elastic network of crosslinked polymer chains during the synthesis [17].) Elastic deformations are described by classical elasticity theory using the Euler strain tensor $\boldsymbol{\varepsilon}$ (compare, for example, ref. [20]). Here, $\varepsilon_{ij} = [\partial_i u_j + \partial_j u_i - (\partial_i u_k)(\partial_j u_k)]/2$, $\mathbf{u}$ being the displacement field.

As an expression for the generalized energy density F, we use [17]

$$\begin{aligned} F = {} & c_1\,\varepsilon_{ij}\varepsilon_{ij} + \frac{1}{2}c_2\,\varepsilon_{ii}\,\varepsilon_{jj} \\ & + \frac{1}{2}D_1\,\tilde{\Omega}_i\tilde{\Omega}_i + D_1^{(2)}\,(\tilde{\Omega}_i\tilde{\Omega}_i)^2 + D_1^{(3)}\,(\tilde{\Omega}_i\tilde{\Omega}_i)^3 \\ & + D_2\,n_i\varepsilon_{ij}\tilde{\Omega}_j + D_2^{nw}\,n_i^{nw}\varepsilon_{ij}\tilde{\Omega}_j^{nw} \\ & + D_2^{(2)}n_i\varepsilon_{ij}\varepsilon_{jk}\tilde{\Omega}_k + D_2^{nw,(2)}n_i^{nw}\varepsilon_{ij}\varepsilon_{jk}\tilde{\Omega}_k^{nw} \\ & - \frac{1}{2}\epsilon_a\,(n_iE_i)^2. \end{aligned} \tag{1}$$

Numerical values of the material parameters c_1, D_1, $D_1^{(2)}$, $D_1^{(3)}$, D_2, D_2^{nw}, $D_2^{(2)}$, and $D_2^{nw,(2)}$ were determined in ref. [17] for a specific homeotropic sample, and we will use these values for our numerical calculations. The last term accounts for the dielectric effects via the dielectric anisotropy ϵ_a [21].

In expression (1) we only included nonlinearities connected with relative rotations. This procedure explicitly excludes intrinsic nonlinear behavior of the network of crosslinked polymer backbones in the absence of director reorientations and relative rotations (there are no terms of cubic or higher order in $\boldsymbol{\varepsilon}$).

4 Shear deformation of prestretched nematic SCLSCEs

We now determine numerically the response of a prestretched nematic SCLSCE to an additional shear of small amplitude δS. For this purpose, we set $\mathbf{E} = \mathbf{0}$ in eq. (1).

According to the procedure of corresponding experiments, we perform the calculation in two steps. First, $\delta S = 0$ and the stretching amplitude A is increased stepwise. For every value of A, we minimize F in eq. (1). That is, we solve the system of equations $\partial F/\partial\vartheta = \partial F/\partial B = \partial F/\partial S = 0$. In this way, we determine ϑ, B, and S as a function of A without an additional external shear δS applied. We include the calculated values for ϑ with increasing prestretching amplitude A in fig. 2. The results coincide with those presented in ref. [17].

Then, for each value of A, the corresponding values of B and S are kept fixed during a second step. We vary, for each value of A, the small amplitude δS of the additional externally imposed shear. For each pair $(\delta S, A)$, we minimize F w.r.t. ϑ only, solving $\partial F/\partial\vartheta = 0$. Experimentally, this procedure corresponds to confining the prestretched sample between the plates of a shear rheometer [15]. Slippage along the plate surfaces is inhibited while the external shear is imposed.

Inserting the results into expression (1), we obtain $F(\delta S, A)$. For each value of A, we find $\partial F/\partial(\delta S)|_{\delta S=0} = 0$, and we can calculate an effective shear modulus for the prestretched sample, $\partial^2 F/\partial(\delta S)^2|_{\delta S=0}$. This effective modulus as a function of the prestretching amplitude A is plotted in fig. 3.

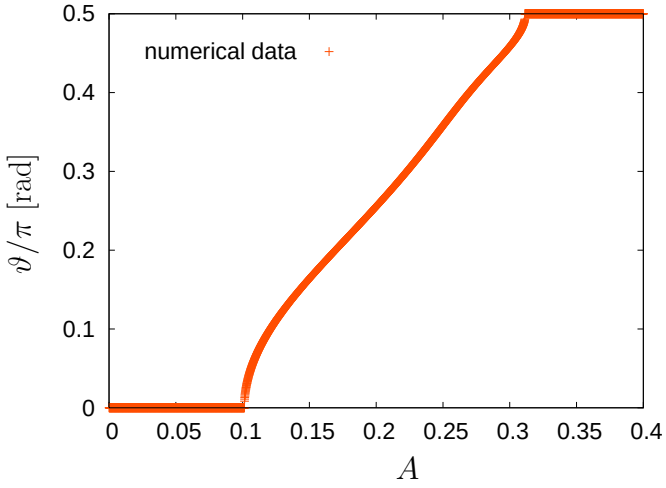

Fig. 2. Angle of director reorientation ϑ as a function of the prestretching amplitude A, without applying an additional external field. In this case, the system is prestretched in a direction perfectly perpendicular to the initial director orientation $\hat{\mathbf{n}}_\mathbf{0}$.

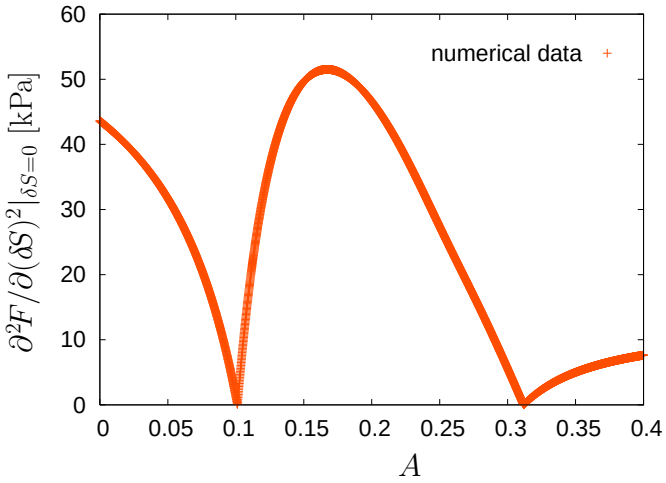

Fig. 3. Effective shear modulus $\partial^2 F/\partial(\delta S)^2|_{\delta S=0}$ as a function of the prestretching amplitude A. Here, the system is prestretched in a direction perfectly perpendicular to the initial director orientation $\hat{\mathbf{n}}_\mathbf{0}$.

At two different stretching amplitudes, the effective modulus tends to zero in fig. 3. These points correspond to the starting point and endpoint of the director reorientation, respectively. If we do not start with a shear amplitude S equilibrated for a certain prestretch A, *e.g.* by setting $S = 0$, the system exerts shear forces. This shifts and modifies the effective modulus in fig. 3. In an experiment (*e.g.* [15]), a similar situation may for example arise if the sample is not completely detached from the corresponding shear plates, while the prestretching amplitude A is being changed.

As a technical check of correctness, we verified the invariance of our numerical results under the symmetry transformation $(\vartheta, \delta S) \to (-\vartheta, -\delta S)$.

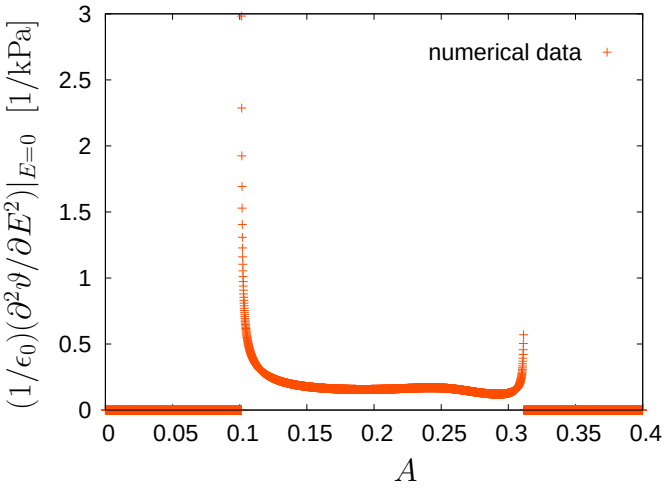

Fig. 4. Reorientability $\partial^2\vartheta/\partial E^2|_{E=0}$ as a function of the prestretching amplitude A, where $\mathbf{E}\|\hat{\mathbf{z}}$ and $\vartheta > 0$. In this example, we set $\epsilon_a/\epsilon_0 = 2$. The system is prestretched in a direction perfectly perpendicular to the initial director orientation $\hat{\mathbf{n}}_\mathbf{0}$.

5 Electric and magnetic field induced director reorientation in prestretched nematic SCLSCEs

Although we only consider electric fields $\mathbf{E}$ in the following, the reasoning is the same for external magnetic fields $\mathbf{H}$. In the latter case, we must make the replacements "$\mathbf{E} \to \mathbf{H}$" and "$\epsilon_a \to \chi_a$", where χ_a is the diamagnetic anisotropy [21].

We now perform a one-step minimization of F. That is, for each given pair $(\mathbf{E}, A)$, we solve the system of equations $\partial F/\partial\vartheta = \partial F/\partial B = \partial F/\partial S = 0$. Thus we obtain $F(\mathbf{E}, A)$.

For each value of A, we find $\partial\vartheta/\partial E|_{E=0} = 0$. Therefore, we take the second derivative $\partial^2\vartheta/\partial E^2|_{E=0}$ to measure the reorientability of the director $\hat{\mathbf{n}}$ for a given stretching amplitude A. An example of $\partial^2\vartheta/\partial E^2|_{E=0}$ as a function of A for $\mathbf{E}\|\hat{\mathbf{z}}$ and $\vartheta > 0$ is plotted in fig. 4. We obtain the same curve for a reorientation $\vartheta < 0$, with the sign of $\partial^2\vartheta/\partial E^2|_{E=0}$ reversed. Furthermore, $\mathbf{E}\|\hat{\mathbf{x}}$ results in identical curves, with reversed signs of $\partial^2\vartheta/\partial E^2|_{E=0}$, respectively.

Strikingly, in fig. 4 we find apparent divergences of the reorientability at the critical values of A. The first apparent divergence takes place at $A = A_c$, where the director reorientation starts ($\vartheta = 0_+$). The second one coincides with the completion of director reorientation ($\vartheta = \pi_-/2$).

We show a fit of a curve $\propto (A - A_c)^x$ to the region $\vartheta \gtrsim 0_+$ in fig. 5. The best result was obtained for $x = -0.474$ and $A_c = 0.1031$, which reproduces the curve in an interval of remarkable width. An exponent $x = -0.5$ still leads to considerable agreement. In order to better understand this behavior, we can reproduce it from expression (1) in a more analytical approach. For this purpose, we solve the equations $\partial F/\partial B = \partial F/\partial S = 0$ w.r.t. B and S and introduce the resulting expressions into $\partial F/\partial\vartheta = 0$. In the case that either $\mathbf{E}\|\hat{\mathbf{x}}$ or $\mathbf{E}\|\hat{\mathbf{z}}$, we find an equation

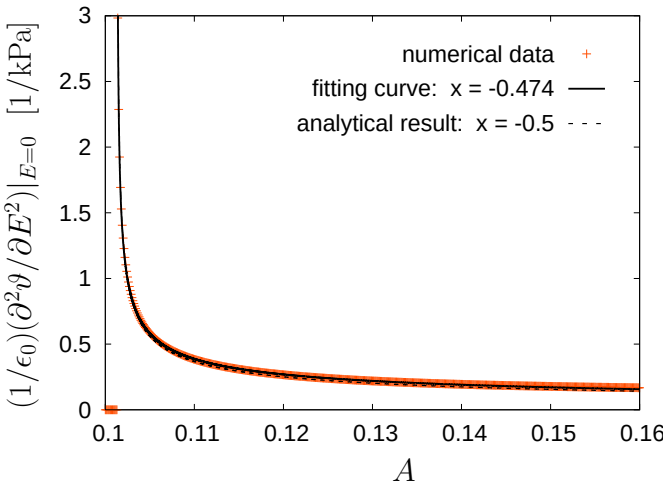

Fig. 5. Reorientability $\partial^2\vartheta/\partial E^2|_{E=0}$ fitted in the region $\vartheta \gtrsim 0_+$ by a curve $\propto (A - A_c)^x$. Again, $\epsilon_a/\epsilon_0 = 2$ and the prestretching direction is oriented perfectly perpendicular to $\mathbf{\hat{n}_0}$.

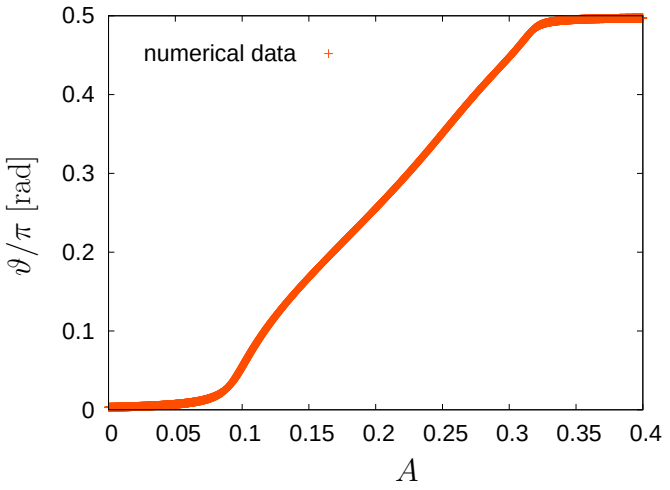

Fig. 6. Angle of director reorientation ϑ as a function of the prestretching amplitude A, without applying an additional external field. Here, the initial director orientation $\mathbf{\hat{n}_0}$ slightly deviates from the perfectly perpendicular orientation $\|\hat{\mathbf{x}}$ by an angle of 0.01 rad (0.57°).

for ϑ of the form

$$0 = \vartheta\{a(A - \tilde{A}_c) + g\vartheta^2\} + \mathcal{O}(\vartheta^5). \qquad (2)$$

Here, higher orders of A have been neglected. a, $\tilde{A}_c$, and g are combinations of the material parameters contained in expression (1). Besides, $\tilde{A}_c$ and g are functions of $E_x^2 - E_z^2$, where we call $A_c = \tilde{A}_c(E = 0)$. For $E = 0$, this leads to the very simple picture of a strain induced forward bifurcation for the reorientation angle ϑ. The branches of the bifurcation are described by $\vartheta = 0$ and $\vartheta \propto \pm(A - A_c)^{0.5}$.

As a further result, we obtain $\partial^2\vartheta/\partial E^2|_{E=0} \propto \pm(A - A_c)^{-0.5}$, where an additional term $\propto (A - A_c)^{0.5}$ was neglected. This behavior is reflected by the fitting curves in fig. 5. Furthermore, we find $\partial^2\vartheta/\partial E_x^2|_{E=0} = -\partial^2\vartheta/\partial E_z^2|_{E=0}$, in accordance with our numerical results.

We performed the same fitting procedure also for the region $\vartheta \lesssim \pi_-/2$. There, we found a behavior characterized by an exponent $x = -0.449$. The corresponding fitting curve represents the numerical data points in a considerably smaller interval. Besides, the width of this interval becomes rather limited for an exponent $x = -0.5$. This reflects the fact that the approximation of neglecting higher order terms in $A(\approx 0.3)$ becomes less reliable for $\vartheta \lesssim \pi_-/2$. Therefore, the range of validity of an equation analogous to eq. (2) is more limited in the region $\vartheta \lesssim \pi_-/2$ and higher order terms in A would have to be included for a better fit.

The reorientability of the director $\partial^2\vartheta/\partial E^2|_{E=0}$ diverges at the same points where the effective shear modulus $\partial^2 F/\partial(\delta S)^2|_{\delta S=0}$ tends to zero. This agrees with the fact that shear deformations and director reorientations are linearly related in nematic SCLSCEs [13,22] (see sect. 7 for further discussion).

6 Oblique stretching

In the previous sections we considered the nematic SCLSCE to be stretched exactly perpendicularly to the initial director orientation $\mathbf{\hat{n}_0}$. However, slight deviations from this condition already change dramatically the corresponding results. As an example, we investigate a very small deviation of the initial director orientation $\mathbf{\hat{n}_0}$ from the perfectly perpendicular orientation $\|\hat{\mathbf{x}}$ by an angle of only 0.01 rad (0.57°). For this case, the angle of director reorientation ϑ is plotted as a function of A in fig. 6.

Figs. 7 and 8 show the corresponding effective shear modulus $\partial^2 F/\partial(\delta S)^2|_{\delta S=0}$ and the director reorientability $\partial^2\vartheta/\partial E^2|_{E=0}$, respectively. Both quantities now remain nonzero and finite. This scenario follows from an imperfect bifurcation for the angle of director reorientation in the oblique case (fig. 6). In contrast, a perfect forward bifurcation underlies the results of figs. 2, 3, and 4 (note the difference in scales between the ordinates of figs. 4 and 8; see also [17]). An experimental curve similar to the curve in fig. 7 has been presented before [16], where a slightly oblique stretching was imposed for intrinsic technical reasons.

7 Discussion

Above, for the case of exactly perpendicular stretching, we observed that the effective shear modulus $\partial^2 F/\partial(\delta S)^2|_{\delta S=0}$ tends to zero at the same points where the reorientability of the director $\partial^2\vartheta/\partial E^2|_{E=0}$ diverges. The physical background of this scenario is connected with the bifurcation behavior of the system at the respective stretching amplitudes. At $A = A_c$, the initial director orientation ($\vartheta = 0$) becomes unstable w.r.t. a solution of finite director reorientation $0 < |\vartheta| < \pi/2$ (see fig. 2). Likewise, when we start at high stretching amplitudes A and then decrease A,

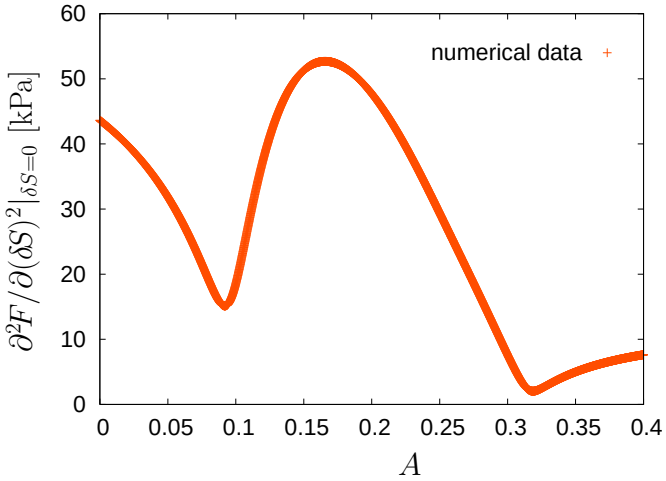

Fig. 7. Effective shear modulus $\partial^2 F/\partial(\delta S)^2|_{\delta S=0}$ as a function of the prestretching amplitude A. The initial director orientation $\hat{\mathbf{n}}_\mathbf{0}$ slightly deviates from the perfectly perpendicular orientation $\|\hat{\mathbf{x}}$ by an angle of 0.01 rad (0.57°).

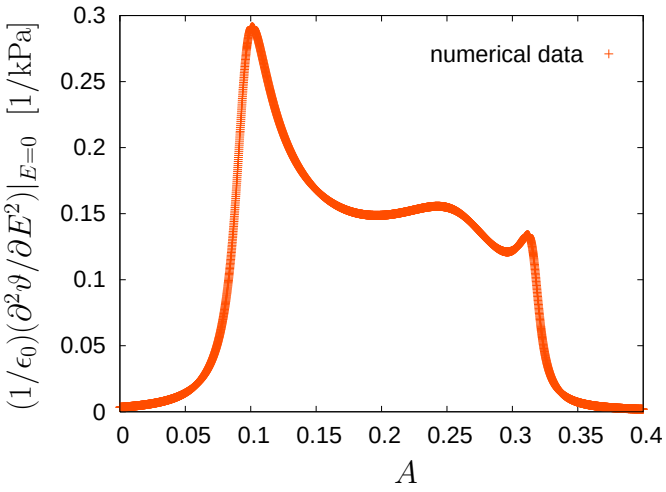

Fig. 8. Reorientability $\partial^2\vartheta/\partial E^2|_{E=0}$ as a function of the prestretching amplitude A ($\epsilon_a/\epsilon_0 = 2$). Again, the initial director orientation $\hat{\mathbf{n}}_\mathbf{0}$ slightly deviates from the perfectly perpendicular orientation $\|\hat{\mathbf{x}}$ by an angle of 0.01 rad (0.57°).

the reoriented state $|\vartheta| = \pi/2$ becomes unstable w.r.t. the intermediate solution $0 < |\vartheta| < \pi/2$. This leads to the second bifurcation behavior at $|\vartheta| = \pi_-/2$ (see fig. 2).

The reorientation of the director is initiated by the coupling of the director orientation to the external stretching deformation. This coupling is mediated by relative rotations (the D_2-, D_2^{nw}-, $D_2^{(2)}$-, $D_2^{nw,(2)}$-terms) in eq. (1). Due to the process of synthesizing the materials, however, the reorientation of the director $\hat{\mathbf{n}}$ w.r.t. the network of crosslinked polymer chains is hindered (the D_1-, $D_1^{(2)}$-, $D_1^{(3)}$-terms in eq. (1)) [2–5, 17]. This competition leads to the described bifurcation behavior. It also induces the shear deformation S, which in this context acts to reduce the magnitude of energetically expensive director rotations w.r.t. the polymer network [17].

In the vicinity of the bifurcation points the director can easily be reoriented by an external field. This feature can be inferred from the diverging slopes of $\vartheta(A)$ in fig. 2. It is further reflected by the diverging curves in figs. 4 and 5, where the external electric field is used to probe the reorientability. Since director reorientations couple linearly to shear deformations in nematic SCLSCEs [13, 22], the effective shear modulus in fig. 3 decreases to zero when the director reorientability diverges. In contrast, the slope of $\vartheta(A)$ remains finite in the remaining regime, distant from the bifurcation points (see fig. 2). This correspondingly implies a finite reorientability of the director and a nonzero effective shear modulus in this regime.

Next, we note that the shape of the curve for the effective shear modulus $\partial^2 F/\partial(\delta S)^2|_{\delta S=0}$ in fig. 3 has already been predicted before [23] on the basis of a different model [24]. Furthermore, a similar curve has been obtained using a semi-microscopic model based on rubber elasticity [25]. Very often, the nonlinear behavior of nematic SCLSCEs, *i.e.* a plateau-like stress-strain relation at finite prestretch with a vanishing effective elastic modulus at the beginning and end of the plateau, is called "semi-softness" [24, 26]. It refers to the notion of "ideal softness", where the stress-strain plateau is of zero height and starts at zero prestretch with the effective elastic modulus being exactly zero everywhere along the plateau (and even in the linear regime at zero prestretch). This ideal Nambu-Goldstone scenario, however, does not take place in real nematic SCLSCEs. The smallness of $A_c \approx 0.1$, the actual prestretch amplitude for the onset of the plateau, is then used to view the real behavior as almost ideal or "semisoft".

We have demonstrated that corresponding results are also derived in a general nonlinear elastic framework. The latter includes nonlinear relative rotations without any assumption or reference to a small parameter in terms of the linear elastic modulus nor in terms of A_c. In this framework, a similar scenario (plateau-like stress-strain relation at finite prestretch with a vanishing effective elastic shear modulus at the beginning and end of the plateau) is obtained even if A_c approaches unity. An example of this kind is displayed in fig. 9, where for demonstration we chose different numerical values for the material parameters ($c_1 = 121.0$ kPa, $D_1 = 30.0$ kPa, $D_1^{(2)} = 3.5$ kPa, $D_1^{(3)} = 2.9$ kPa, $D_2 = 0.0$ kPa, $D_2^{nw} = 0.0$ kPa, $D_2^{(2)} = -55.5$ kPa, and $D_2^{(2),nw} = -32.0$ kPa). We note that $A = 1$ corresponds to an infinite stretching deformation. Therefore we view the pronounced elastic properties of real nematic SCLSCEs as a manifestation of the profoundly nonlinear elastic properties of the materials, rather than due to the vicinity of a hypothetical ideal state.

For a more detailed comparison with other approaches, we note the following. Concentrating only on the quadratic terms in the generalized energy density, we obtain as a condition of thermodynamic stability that $4c_1D_1 - (D_2 + D_2^{nw})^2 > 0$ [17]. As explained in ref. [26], the transition from "semi-softness" to "ideal softness" in the linear regime corresponds to the case where the latter expression vanishes, $4c_1D_1 - (D_2 + D_2^{nw})^2 \to 0$. On the one hand, this

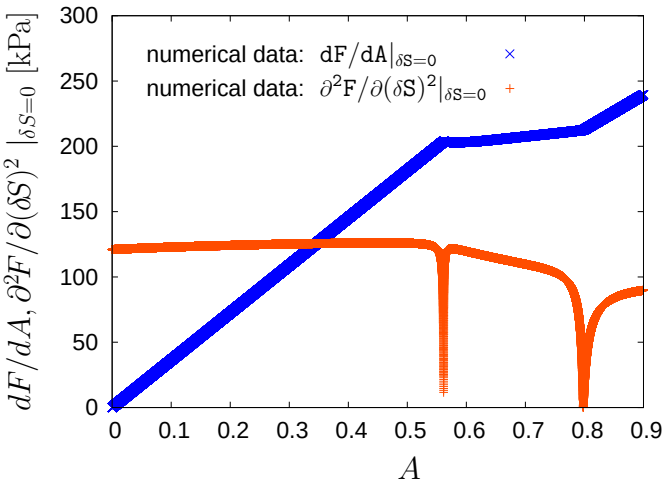

Fig. 9. Example of a stress-strain curve $dF/dA|_{\delta S=0}(A)$, calculated by our model for the geometry depicted in fig. 1(a) for a different set of material parameters. In this case, the process of director reorientation and the corresponding decrease in the slope of the stress-strain curve occur at comparatively large prestretching amplitudes A. Again, the effective elastic shear modulus $\partial^2 F/\partial(\delta S)^2|_{\delta S=0}$ tends to zero in the vicinity of the points where the director reorientation starts and ends.

may occur by $D_1 \to 0$, $D_2 \to 0$, and $D_2^{nw} \to 0$. This, however, implies that relative rotations have no meaning, or, in other words, that the director has no memory of its initial orientation. Definitely, this is not true for real nematic SCLSCEs. On the other hand, the condition may be satisfied by $4c_1 D_1 = (D_2 + D_2^{nw})^2$ without D_1 vanishing. As a result, one recovers in the linear regime the vanishing shear modulus predicted by the theory of "soft elasticity" when the shear plane contains the director [26, 27]. However, the statement becomes problematic when deformations and reorientations are not correspondingly small (compare also ref. [28]).

In our approach, a scenario of "softness" can be recovered in the following way for the complete reorientation process. One neglects the memory of the initial director orientation. Therefore the variables of relative rotation become meaningless and one sets $D_1 = D_1^{(2)} = D_1^{(3)} = D_2 = D_2^{nw} = D_2^{(2)} = D_2^{nw,(2)} = 0$. A supplement to the elastic part of the energy leads to $F = c_1 \varepsilon_{ij}\varepsilon_{ij} + c_2 \varepsilon_{ii}\varepsilon_{jj}/2 + \tilde{c}_5 n_i \varepsilon_{ij} n_j$. If we choose $\tilde{c}_5 < 0$, we recover for our geometry the above-mentioned scenario of "ideal softness": zero height of the stress-strain plateau during the reorientation process, starting at zero prestretch. Here, the additional term $\tilde{c}_5 n_i \varepsilon_{ij} n_j$ acts as an intrinsic force of deformation that arises from the nematic state of the material (compare refs. [28, 29] for related approaches). Real nematic SCLSCEs, however, do not show the scenario of "ideal softness", therefore we did not include the corresponding term with the coefficient $\tilde{c}_5$.

We would like to include three further remarks. First, we have demonstrated in ref. [17] that the materials show an additional intrinsic nonlinear stress-strain behavior due to nonlinear elasticity. This kind of nonlinear behavior is not connected to director reorientations. It arises simply from straining the crosslinked polymer network. Nevertheless, it influences significantly the overall stress-strain behavior of the elastomers [17]. These nonlinear properties, which we have neglected above, could force the effective shear modulus $\partial^2 F/\partial(\delta S)^2|_{\delta S=0}$ to remain at a finite, nonzero level. Secondly, the finiteness of real samples renders the lateral boundaries to move and change shape during stretching. That leads to deviations from the bulk director orientation close to the boundaries. The conditions for the effective shear modulus to vanish might therefore not be met close to the boundaries. Furthermore, within the sample, the critical stretching amplitude A_c may vary on a macroscopic length scale due to spatial heterogeneities. If, in an experiment, one simultaneously probes such macroscopic regions of different A_c, the observed effective shear modulus will not vanish.

Our results are interesting from an experimental and an applied point of view. Since director reorientations in nematic elastomers are connected to elastic deformations, they are candidates for the potential use as actuators [6,10,30–32]. So far, only swollen nematic elastomers show a considerable director reorientation at reasonably low external electric field amplitudes [3,6,10,11]. However, fine-tuned prestretching of nematic elastomers may allow a considerable electric field induced director reorientation and resulting elastic deformations also for dry materials.

The authors thank Philippe Martinoty and Kenji Urayama for stimulating discussions. A.M.M. and H.R.B. thank the Deutsche Forschungsgemeinschaft through the Forschergruppe FOR608 'Nichtlineare Dynamik komplexer Kontinua' and the Deutscher Akademischer Austauschdienst (312/pro-ms) through PROCOPE for partial support of this work. A.M.M. acknowledges partial support by the ENB 'Macromolecular Science'.

References

1. H. Finkelmann, H.-J. Kock, G. Rehage, Makromol. Chem., Rapid Commun. **2**, 317 (1981).
2. H.R. Brand, K. Kawasaki, Macromol. Rapid Commun. **15**, 251 (1994).
3. D.-U. Cho, Y. Yusuf, P.E. Cladis, H.R. Brand, H. Finkelmann, S. Kai, Jap. J. Appl. Phys. **46**, 1106 (2007).
4. J. Küpfer, H. Finkelmann, Makromol. Chem., Rapid Commun. **12**, 717 (1991).
5. J. Küpfer, H. Finkelmann, Macromol. Chem. Phys. **195**, 1353 (1994).
6. K. Urayama, S. Honda, T. Takigawa, Macromol. **38**, 3574 (2005).
7. I. Kundler, H. Finkelmann, Macromol. Rapid Commun. **16**, 679 (1995).
8. I. Kundler, H. Finkelmann, Macromol. Chem. Phys. **199**, 677 (1998).
9. K. Urayama, R. Mashita, I. Kobayashi, T. Takigawa, Macromol. **40**, 7665 (2007).
10. Y. Yusuf, J.H. Huh, P.E. Cladis, H.R. Brand, H. Finkelmann, S. Kai, Phys. Rev. E **71**, 061702 (2005).

11. K. Urayama, S. Honda, T. Takigawa, Macromol. **39**, 1943 (2006).
12. P. Stein, N. Aßfalg, H. Finkelmann, P. Martinoty, Eur. Phys. J. E **4**, 255 (2001).
13. P. Martinoty, P. Stein, H. Finkelmann, H. Pleiner, H.R. Brand, Eur. Phys. J. E **14**, 311 (2004).
14. D. Rogez, G. Francius, H. Finkelmann, P. Martinoty, Eur. Phys. J. E **20**, 369 (2006).
15. P. Martinoty, presentation at the *International Liquid Crystal Elastomer Conference*, Ljubljana, 2007.
16. A. Petelin, M. Čopič, presentations at the *European Conference on Liquid Crystals*, Colmar, 2009.
17. A.M. Menzel, H. Pleiner, H.R. Brand, J. Appl. Phys. **105**, 013503 (2009).
18. P.G. de Gennes, in *Liquid Crystals of One- and Two-Dimensional Order*, edited by W. Helfrich, G. Heppke (Springer, Berlin, 1980), pp. 231 ff.
19. H.R. Brand, H. Pleiner, Physica A **208**, 359 (1994).
20. H. Temmen, H. Pleiner, M. Liu, H.R. Brand, Phys. Rev. Lett. **84**, 3228 (2000).
21. P.G. de Gennes, J. Prost, *The Physics of Liquid Crystals* (Clarendon Press, Oxford, 1993).
22. A.M. Menzel, H. Pleiner, H.R. Brand, J. Chem. Phys. **126**, 234901 (2007).
23. T.C. Lubensky, remarks at the *International Liquid Crystal Elastomer Conference*, Ljubljana, 2007.
24. F.F. Ye, T.C. Lubensky, J. Phys. Chem. B **113**, 3853 (2009).
25. J.S. Biggins, E.M. Terentjev, M. Warner, Phys. Rev. E **78**, 041704 (2008).
26. M. Warner, E.M. Terentjev, *Liquid Crystal Elastomers* (Clarendon Press, Oxford, 2003); and references therein.
27. L. Golubović, T.C. Lubensky, Phys. Rev. Lett. **63**, 1082 (1989).
28. T.C. Lubensky, R. Mukhopadhyay, L. Radzihovsky, X. Xing, Phys. Rev. E **66**, 011702 (2002).
29. A. Fukunaga, K. Urayama, T. Takigawa, A. DeSimone, L. Teresi, Macromol. **41**, 9389 (2008).
30. R. Zentel, Liq. Cryst. **1**, 589 (1986).
31. Y. Yusuf, Y. Sumisaki, S. Kai, Chem. Phys. Lett. **382**, 198 (2003).
32. Y. Yu, T. Ikeda, Angew. Chem. Int. Ed. **45**, 5416 (2006).